Inorganic Chemistry
Article

Inorg. Chem. **2010**, *49*, 3737–3745 **3737**
DOI: 10.1021/ic902070q

Synthesis and Characterization of Ruthenium(II)−Pyridylamine Complexes with Catechol Pendants as Metal Binding Sites

Takahiko Kojima,*,† Norihisa Hirasa,‡ Daisuke Noguchi,§ Tomoya Ishizuka,† Soushi Miyazaki,‡ Yoshihito Shiota,∥ Kazunari Yoshizawa,∥ and Shunichi Fukuzumi*,‡,⊥

†*Department of Chemistry, Graduate School of Pure and Applied Sciences, University of Tsukuba, Tsukuba, Ibaraki 305-8571,* ‡*Department of Material and Life Science, Graduate School of Engineering, Osaka University and SORST (JST), 2-1 Yamada-oka, Suita, Osaka 565-0871,* §*Department of Chemistry, Graduate School of Sciences, and* ∥*Institute for Materials Chemistry and Engineering, Kyushu University, Hakozaki, Higashi-Ku, Fukuoka 812-8581, Japan, and* ⊥*Department of Bioinspired Science, Ewha Womans University, Seoul, 120-750, Korea*

Received October 20, 2009

A novel tris(2-pyridylmethyl)amine (TPA) derivate having two catechol moieties linked by amide linkages at the 6-positions of two pyridyl groups was synthesized. The ligand, *N*,*N*-bis[6-{3,4-(dihydroxy)benzamide}-2-pyridyl-methyl]-*N*-(2-pyridylmethyl)amine (Cat_2-TPA; **L2**), and its precursor, *N*,*N*-bis[6-{3,4-bis(benzyloxy)-benzamide}-2-pyridyl-methyl]-*N*-(2-pyridylmethyl)-amine (($Bn_2Cat)_2$-TPA; **L1**), formed stable ruthenium(II) complexes, [RuCl(**L2**)]PF_6 (**2**) and [RuCl(**L1**)]PF_6 (**1**), respectively. The crystal structure of [RuCl(**L2**)]Cl (**2′**) was determined by X-ray crystallography to show two isomers in terms of the orientation of one catechol moiety. In complex **2**, the ligand bearing catechols acts as a pentadentate ligand involving coordination of one of the amide oxygen atoms in addition to that of the tetradentate TPA moiety and two metal-free catechol moieties as metal-binding sites. The coordination of **L2** results in the preorganization of the two catechols to converge them to undergo intramolecular $\pi-\pi$ interactions. The ^{1}H NMR spectrum of **2** in DMSO-d_6 revealed that only one isomer was present in the solution. This selective formation could be ascribed to the formation of an intramolecular hydrogen-bonding network among the hydroxyl groups of the catechol moieties, as suggested by X-ray analysis. This intramolecular hydrogen bonding could differentiate the pK_a values of the hydroxy groups of the catechol moieties into three kinds, as indicated by spectroscopic titration with tetramethylammonium hydroxide (TMAOH) in DMF. The complexation of **2** with other metal ions was also examined. The reaction of **2** with [$Cu(NO_3)_2$(TMEDA)] (TMEDA = *N*,*N*,*N*′,*N*′-tetramethylethylenediamine) in methanol allowed us to observe the selective formation of a binuclear complex, [RuCl(**L2**$^{2-}$){Cu(TMEDA)}]PF_6 (**3**), which was characterized by ESI-MS, UV−vis, and ESR spectroscopies. Its ESR spectrum in methanol suggested that the coordination of the Cu(II)-TMEDA unit to the converged catechol moieties would be different from conventional κ^2-*O*,*O*′:η^2-coordination: it exhibits a novel bridging coordination mode, bis-κ^1-*O*:η^1-coordination, to form the binuclear Ru(II)−Cu(II) complex.

Introduction

Catechol (1,2-dihydroxybenzene; H_2Cat) and its derivatives have been known to form stable complexes with metal ions.[1] Usually, catechols coordinate to metal ions through the two oxygen atoms via deprotonation as dianionic and bidentate catecholato ligands to form a stable five-membered chelate ring.[1] Nature utilizes this characteristic of catechol moieties in siderophores, which play indispensable roles in the uptake and transport of metal ions.[2,3] In the structure of enterobactin for the uptake and transport of iron, as a representative of natural siderophores, catechol moieties are organized and converged by a cyclic triester backbone to facilitate the strong binding of the Fe(III) ion.[4]

*To whom correspondence should be addressed. E-mail: kojima@chem.tsukuba.ac.jp (T.K.), fukuzumi@chem.eng.osaka-u.ac.jp (S. F.).

(1) (a) Pierpont, C. G.; Buchanan, R. M. *Coord. Chem. Rev.* **1981**, *38*, 45–87. (b) Pierpont, C. G. *Coord. Chem. Rev.* **2001**, *219−221*, 415–433. (c) Sever, M. J.; Wilker, J. J. *Dalton Trans.* **2004**, 1061–1072. (d) Albrecht, M.; Janser, I.; Fröhlich, R. *Chem. Commun.* **2005**, 157–165. (e) Jang, H. G.; Cox, D. D.; Que, L., Jr. *J. Am. Chem. Soc.* **1991**, *113*, 9200–9204. (f) Kurihara, M.; Kato, N.; Kojima, T.; Ishii, Y.; Matsuda, Y. *Inorg. Chem.* **1995**, *34*, 4888–4895. (g) Shavaleev, N. M.; Davles, E. S.; Adams, H.; Best, J.; Weinstein, J. A. *Inorg. Chem.* **2008**, *47*, 1532–1547. (h) Bruijnincx, P. C. A.; Viciano-Chumillas, M.; Lutz, M.; Spek, A. L.; Reedjik, J.; van Koten, G.; Gebbink, J. M. K. *Chem.−Eur. J.* **2008**, *14*, 5567–5576.

(2) For Fe: Crosa, J. H.; Walsh, C. T. *Microbiol. Mol. Biol. Rev.* **2002**, *66*, 223–249.

(3) For Mo: Bellenger, J.-P.; Arnaud-Neu, F.; Asfari, Z.; Myneni, S. C. B.; Stiefel, E. I.; Kraepiel, A. M. L. *J. Biol. Inorg. Chem.* **2007**, *12*, 367–376.

(4) Raymond, K. N.; Dertz, E. A.; Kim, S. S. *Proc. Natl. Acad. Sci. U. S. A.* **2003**, *100*, 3584–3588.

Published on Web 03/23/2010

Scheme 1. Preorganization of Catechol Moieties by Metal Complexation to Form a *Metal−Complex Ligand*

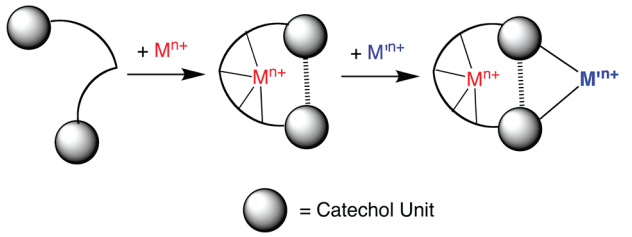

The combination of catechol moieties with other metal binding sites having different characters such as pyridylamines, that is "ditopic", offers more than two different coordination environments in one molecule. This type of ditopic ligand is useful for selective coordination of metal ions to favorable sites depending on the characteristics of the metal ions, giving rise to well-defined heterometallic multinuclear metal complexes to develop new integrated functionality.[5] So far, it has been reported that catechol moieties have been linked to, for example, 2,2′-bipyridine,[6] 2,2′;6′,2″-terpyridine,[6] and macrocyclic ligands[7] to afford ditopic ligands.

In order to develop a new strategy to construct heterometallic multinuclear complexes, we designed a novel ditopic ligand using a flexible multidentate scaffold that links to catechol moieties via an amide linkage. Complexation of an appropriate metal ion to the flexible multidentate site fixes the conformation and configuration of the ligand by virtue of a template effect of the metal ions to preorganize the geometry of the catechol sites which can enjoy free orientations in solution, as shown in Scheme 1, in place of the organic backbones observed in natural siderophores. Such preorganization of the catechol moieties allows us to employ a *metal−complex ligand* with catechols as metal-binding sites. On the basis of this strategy, we can create novel multinuclear metal complexes with multiredox systems involving mutual electronic interactions among those redox centers, including redox-noninnocent catechol moieties.[8]

We have reported on the synthesis and characterization of Ru(II) complexes having tris(2-pyridylmethyl)amine (TPA) derivatives with two functional groups via amide linkages as ligands.[9,10] In those complexes, the TPA derivatives coordinate to the Ru(II) centers as pentadentate ligands involving coordination of the amide oxygen that is stabilized by an intramolecular hydrogen bonding.[9,10] The amide oxygen coordination and the intramolecular hydrogen bonding result in the convergence of the functional groups to allow them to undergo intramolecular noncovalent interactions such as $\pi-\pi$ interactions.[9] Thus, we applied this methodology to the preorganization of catechol moieties linked to the TPA ligand via an amide linkage to construct a novel metal−complex ligand with converged catechol moieties.

In this paper, we describe the synthesis and characterization of a novel TPA derivative having two catechol units via amide linkages and its Ru(II) complex. In addition, the complexation of the Ru(II) complex with a Cu(II)-diamine unit was also studied to propose a novel coordination mode of converged catechol moieties.

Experimental Section

Materials and Apparatus. Dichloromethane (CH_2Cl_2), carbon tetrachloride (CCl_4), triethylamine (NEt_3), and tetrahydrofuran (THF) were distilled over CaH_2 under N_2 prior to use. Chemicals such as dimethylformamide (DMF) were distilled and stored under N_2. *N*-Bromosuccinimide (NBS) was recrystallized from hot water prior to use. Other chemicals were used as received. *N*,*N*-Bis(6-amino-2-pyridylmethyl)-*N*-(2-pyridylmethyl)amine·3HCl (diamino-TPA·3HCl) was prepared as previously reported.[9b] The dichloro(*p*-cymene)-ruthenium(II) dimer was purchased from Aldrich and used without further purification. [$Cu(NO_3)_2$(TMEDA)] (TMEDA = *N*,*N*,*N*′*N*′-tetramethylethylenediamine) was synthesized as reported.[11]

UV−vis absorption spectra were recorded on a Jasco Ubest-55 UV/vis spectrophotometer at room temperature. All NMR measurements were carried out on JEOL-JNM-AL300 and Bruker AVANCE 400 spectrometers at 25 °C. IR spectra of solid samples were recorded on a Thermo Nicolet NEXUS 870 FT-IR instrument using 2 cm^{-1} standard resolution at ambient temperature in KBr pellets. ESI-MS spectra were measured on a Perkin-Elmer SCIEX API 150 EX mass spectrometer in positive detection mode, equipped with an ion spray interface. The sprayer was held at a potential of +5.0 kV, and compressed N_2 was employed to assist liquid nebulization. The orifice potential was maintained at +20 V.

Synthesis of Benzyl 3,4-Bis(benzyloxy)benzoate.[12] A solution of proto-catechuic acid (10.0 g, 0.065 mol), benzyl chloride (30 mL, 0.26 mol), and Na_2CO_3 (45.0 g, 0.42 mol) in DMF (150 mL) was refluxed for 48 h. The mixture was filtered, and the filtrate was dried up under reduced pressure. The residue was purified by column chromatography on a silica gel (CH_2Cl_2, R_f = 0.8). A white liquid of the compound was obtained. The yield was 85% (23.5 g). ^{1}H NMR ($CDCl_3$, δ (ppm)): 5.20 (s, 2H, Bn-CH_2), 5.23 (s, 2H, Bn-CH_2), 5.32 (s, 2H, Bn-CH_2), 6.93 (d, 1H, J = 7 Hz, *H*5), 7.31−7.47 (m, 15H, Bn-Ph), 7.66−7.68 (m, 2H, *H*2, *H*6). MALDI−TOF MS: m/z = 446.90 (M − 2H$^+$).

Synthesis of 3,4-Bis(benzyloxy)benzoic Acid.[12] A solution of benzyl 3,4-bis(phenylmethoxy)benzoate (10 g, 30 mmol) and NaOH (2.88 g, 72.0 mmol) in 11:5 v/v methanol/water (160 mL) was refluxed for 2 h and then cooled. After filtration, the filtrate was dried up under reduced pressure. Concentrated HCl was added, and then a white solid of the compound was obtained. The yield was 92% (7.2 g). ^{1}H NMR (($CD_3)_2CO$, δ (ppm)): 5.21 (s, 2H, Bn-CH_2), 5.25 (s, 2H, Bn-CH_2), 7.15 (d, 1H, J = 8 Hz, *H*5), 7.30−7.40 (m, 6H, Bn-*Ph*), 7.50−7.53 (m, 4H, Bn-*Ph*), 7.63 (d, 1H, J = 2 Hz, *H*2), 7.67 (dd, 1H, J = 8, 2 Hz, *H*6). IR (KBr): ν = 1687 (C═O), 1677, 1601, 1306, 1277, 1225 cm^{-1}.

Synthesis of 3,4-Bis(benzyloxy)benzoyl Chloride.[12] To a degassed solution of 3,4-bis(phenylmethoxy)benzoic acid (1 g,

(5) Guerra, K. P.; Delgado, R. *Dalton Trans.* **2008**, 539–550.
(6) Shukla, A. D.; Whittle, B.; Bajaj, H. C.; Das, A.; Ward, M. D. *Inorg. Chim. Acta* **1999**, *285*, 89–96.
(7) Jonasdottir, S.; Kim, C.-G.; Kampf, J.; Coucouvanis, D. *Inorg. Chim. Acta* **1996**, *243*, 255–270.
(8) (a) Piepont, C. G. *Coord. Chem. Rev.* **2001**, *216−217*, 99–125. (b) Evangelio, E.; Ruiz-Molina, D. *Eur. J. Inorg. Chem.* **2005**, 2957–2971. (c) Shimazaki, Y.; Kabe, R.; Huth, S.; Tani, F.; Naruta, Y.; Yamauchi, O. *Inorg. Chem.* **2007**, *46*, 6083–6090. (d) Ohtsu, H.; Tanaka, K. *Chem.−Eur. J.* **2005**, *11*, 3420–3426.
(9) (a) Kojima, T.; Hayashi, K.; Matsuda, Y. *Chem. Lett.* **2000**, 1008–1009. (b) Kojima, T.; Hayashi, K.; Matsuda, Y. *Inorg. Chem.* **2004**, *43*, 6793–6804. (c) Kojima, T.; Miyazaki, S.; Hayashi, K.; Shimazaki, Y.; Tani, F.; Naruta, Y.; Matsuda, Y. *Chem.−Eur. J.* **2004**, *10*, 6402–6410. (d) Kojima, T.; Hayashi, K.; Tachi, Y.; Naruta, Y.; Suzuki, T.; Uezu, K.; Shiota, Y.; Yoshizawa, K. *Bull. Chem. Soc. Jpn.* **2005**, *78*, 2152–2158. (e) Kojima, T.; Noguchi, D.; Nakayama, T.; Inagaki, Y.; Shiota, Y.; Yoshizawa, K.; Ohkubo, K.; Fukuzumi, S. *Inorg. Chem.* **2008**, *47*, 886–895.
(10) Jitsukawa, K.; Oka, Y.; Yamaguchi, S.; Masuda, H. *Inorg. Chem.* **2004**, *43*, 8119–8129.
(11) Pavkovic, S. F.; Miller, D.; Brown, J. N. *Acta Crystallogr.* **1977**, *B33*, 2894–2896.
(12) Wang, W.-L.; Chai, S. C.; Ye, Q.-Z. *Bioorg. Med. Chem. Lett.* **2009**, *19*, 1080–1083.

Chart 1

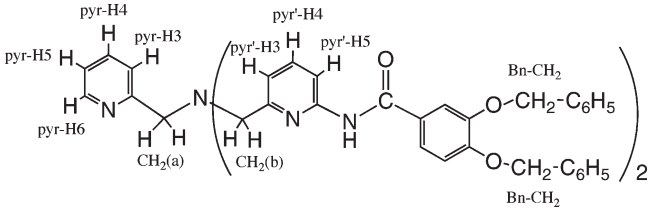

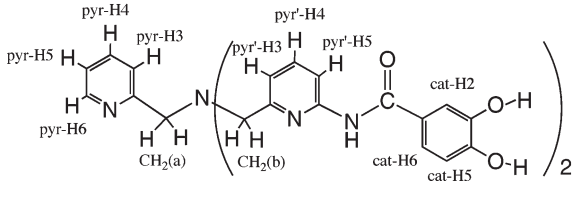

2.84 mmol) in CH_2Cl_2 (10 mL) was added oxalyl dichloride (10 mL, 0.3 mol) under N_2. The mixture was stirred for 12 h at room temperature. After filtration, the filtrate was dried up under reduced pressure, and then a white solid of the acid chloride was obtained. The yield was 81% (0.85 g). The obtained compound was used without further purification. IR (KBr, cm^{-1}): ν = 1739 (C═O), 1677, 1590, 1515, 1277, 1225.

Synthesis of *N*,*N*-Bis[6-*N*,*N*-bis{3,4-bis(benzyloxy)-benzamide}-2-pyridyl-methyl]-*N*-(2-pyridylmethyl)amine ($(Bn_2Cat)_2$-TPA, L1). To a degassed solution of 3,4-bis(phenylmethoxy)benzoyl chloride (2.98 g, 8.47 mmol) and NEt_3 (12 mL) in THF (36 mL) was added diamino-TPA·3HCl (1.01 g, 3.13 mmol) in THF (36 mL) dropwise over a period of 30 min under N_2 at 0 °C, and then *N*,*N*-dimethylaminopyridine (DMAP) (0.91 g) was added to the solution. The mixture was refluxed for 14 h and then filtered. The filtrate was dried up under reduced pressure and purified by column chromatography on activated alumina (ethyl acetate, R_f = 0.9), followed by that on silica gel (ethyl acetate → methanol, R_f = 0.1). The ligand was obtained as a white liquid in 50% yield (2.00 g). ESI-MS: *m*/*z* 975.46 ($[M + Na]^+$), 953.42 ($[M + H]^+$). ^{1}H NMR ($CDCl_3$, δ (ppm)): 3.79 (s, 4H, C*H*$_2$(b)), 3.91 (s, 2H, C*H*$_2$(a)), 5.21 (s, 4H, Bn-C*H*$_2$), 5.22 (s, 4H, Bn-C*H*$_2$), 6.96 (d, 2H, *J* = 8.4 Hz, cat-H5), 7.15 (dd, 1H, *J* = 8, 2 Hz, pyr-H5), 7.29−7.39 (m, 14H, cat-H6, pyr′-H3 and Bn-*Ph*), 7.42−7.48 (m, 10H, Bn-*Ph*), 7.55 (d, 1H, *J* = 8 Hz, pyr-H3), 7.61 (d, 2H, *J* = 2 Hz, cat-H2), 7.66 (td, 1H, *J* = 8, 2 Hz, pyr-H4), 7.71 (t, 2H, *J* = 8 Hz, pyr′-H4), 8.19 (d, 2H, *J* = 8 Hz, pyr′-H5), 8.46 (s, 2H, N-*H*), 8.53 (dd, 1H, *J* = 8, 2 Hz, pyr-H6). The numbering of protons is shown in Chart 1.

Synthesis of *N*,*N*-Bis{6-(3, 4-dihydroxybenzamide)-2-pyridyl-methyl}-*N*-(2-pyridylmethyl)amine ($(H_2Cat)_2$-TPA, L2). A degassed solution of **L1** (137 mg, 0.148 mmol) and iodotrimethylsilane (0.5 mL, 4 mmol) in CH_3CN (10 mL) was stirred for 24 h. The reaction was quenched by adding MeOH, and then the reaction mixture was filtered. The filtrate was dried up under reduced pressure, and the residue was washed with diethyl ether and then washed with a small volume of MeOH. The yield was 85% (74 mg). ESI-MS: *m*/*z* 593.14 ($[M + H]^+$). ^{1}H NMR (DMSO-d_6, δ (ppm)): 4.48 (s, 4H, C*H*$_2$(b)), 4.73 (s, 2H, C*H*$_2$(a)), 6.81 (d, 2H, *J* = 8 Hz, cat-H5), 7.26 (d, 2H, *J* = 7 Hz, pyr′-H3), 7.36−7.40 (m, 4H, cat-H2 and -*H*6), 7.53 (dd, 1H, *J* = 8, 6 Hz, pyr-*H*5), 7.70 (d, 1H, *J* = 8 Hz, pyr-*H*3), 7.86 (t, 2H, *J* = 8 Hz, pyr′-*H*4), 7.99−8.05 (m, 3H, pyr-*H*5 and pyr′-*H*5), 8.67 (dd, 1H, *J* = 4, 2 Hz, pyr-*H*6), 10.34 (s, 2H, N-*H*). The numbering of protons is shown in Chart 1.

Synthesis of [RuCl(L1)]PF_6 (1). To a refluxed deep green solution of $RuCl_3 \cdot 3H_2O$ (22.5 mg, 0.0862 mmol) in ethanol (15 mL) was added $(Bn_2Cat)_2$-TPA (**L1**) (80 mg, 0.086 mmol) as a solid, and the mixture was refluxed for 24 h. To the resultant brown solution was added $NaPF_6$ (17.4 mg, 0.104 mmol), and the solution was concentrated to a small volume to obtain a yellow powder of **1**, which was washed with a minimum volume of ethanol and diethyl ether and then dried. The yield was 58% (62.5 mg). Anal. Calcd for $C_{60}H_{52}N_6O_6ClRuPF_6 \cdot 1.5H_2O$: C, 57.12; H, 4.39; N, 6.66. Found: C, 57.06; H, 4.18; N, 6.66. ESI-MS: *m*/*z* 1089.33 ($[M\text{-}PF_6]^+$), 549.21 ($[M\text{-}PF_6\text{-}Cl\text{-}2H{+}2Na]^{2+}$), 527.16 ($[M\text{-}PF_6\text{-}Cl]^{2+}$). ^{1}H NMR ($CD_3CN$, δ (ppm)): 4.34 and 4.47 (ABq, J_{AB} = 18 Hz, C*H*$_2$(a)), 4.64 and 4.95 (ABq, J_{AB} = 15 Hz, C*H*$_2$(b′)), 4.65 and 5.14 (ABq, J_{AB} = 14 Hz, C*H*$_2$(b)), 4.78 (s, 2H, Bn-C*H*$_2$), 5.03 (s, 2H, Bn-C*H*$_2$), 5.08 (s, 2H, Bn-C*H*$_2$), 5.12 (s, 2H, Bn-C*H*$_2$), 6.48 (d, 1H, *J* = 8.8 Hz, cat′-H5), 6.63 (d, 1H, *J* = 8.6 Hz, cat-H5), 6.94 (dd, 1H, *J* = 8.8, 1.5 Hz, cat′-H6), 7.07−7.57 (m, 29H, aromatic), 7.64 (t, 1H, *J* = 8.4 Hz, pyr′-H4), 7.75 (t, 1H, *J* = 8.1 Hz, pyr-H4), 8.43−8.46 (m, 2H, pyr−*H*6 and pyr′-H5), 10.06 (s, 1H, N-*H* of amide (coordinated)), 10.30 (s, 1H, N−*H* of amide (uncoordinated and hydrogen−bonded)). Absorption maxima (λ_{max}, nm): 305 ($\varepsilon = 3.4 \times 10^4\ M^{-1}\ cm^{-1}$), 455 ($\varepsilon = 8.6 \times 10^3\ M^{-1}\ cm^{-1}$).

Synthesis of [RuCl(L2)]PF_6 (2). A solution containing $[RuCl_2(p\text{-cymene})]_2$ (49.2 mg, 0.0804 mmol) and $(H_2Cat)_2$-TPA (**L2**) (100 mg, 0.169 mmol) in methanol (20 mL) was refluxed for 24 h. After filtration, the filtrate was dried up under reduced pressure. The residue was dissolved in a small volume of methanol, and then NH_4PF_6 (16.0 mg, 0.098 mmol) was added. The mixture was concentrated under reduced pressure to obtain a brown precipitate. The precipitate was filtered and washed with CH_3CN and then dried. A reddish orange powder of **2** was obtained. The yield was 56% (40.0 mg). Anal. Calcd for $C_{32}H_{28}N_6O_6ClRuPF_6 \cdot CH_3CN \cdot 4H_2O$: C, 41.42; H, 3.89; N, 10.15. Found: C, 41.36; H, 3.98; N, 9.93. ^{1}H NMR (CD_3CN, δ (ppm)): 4.34 and 4.53 (ABq, J_{AB} = 18 Hz, C*H*$_2$(a)), 4.48 and 4.58 (ABq, J_{AB} = 18 Hz, C*H*$_2$(b)), 4.75 and 4.90 (ABq, J_{AB} = 15 Hz, C*H*$_2$(b′)), 6.10 (s, 1H, cat-H2), 6.39 (d, 1H, *J* = 8.0 Hz, cat-H5), 6.67 (d, 1H, *J* = 8.0 Hz, cat-H5′), 6.94 (dd, 1H, *J* = 8.0, 2.0 Hz, cat-H6), 7.07 (dd, 1H, *J* = 8.0, 2.0 Hz, cat′-H6), 7.15−7.26 (m, 6H, aromatics), 7.68 (td, 1H, *J* = 8.0, 2.0 Hz, pyr-H4), 7.76 (t, 1H, *J* = 8.0 Hz, pyr′-H4′), 7.85 (t, 1H, *J* = 8.0 Hz, pyr′-H4), 8.36 (d, 1H, *J* = 8.0 Hz, pyr′-H5), 8.41 (d, 1H, *J* = 8.0 Hz, pyr-H6), 9.81 (s, 1H, N−*H* of amide (uncoordinated and hydrogen−bonded)), 10.05 (s, 1H, N−*H* of amide (coordinated)). ESI-MS: *m*/*z* 729.2 ($[M\text{-}PF_6]^+$), 347.1 ($[M\text{-}PF_6\text{-}Cl]^{2+}$). Absorption maxima ($\lambda_{max}$, nm): 311 ($\varepsilon = 3.7 \times 10^4\ M^{-1}\ cm^{-1}$), 442 ($\varepsilon = 9.6 \times 10^3\ M^{-1}\ cm^{-1}$)

Synthesis of [RuCl($(HCat)_2$-TPA){Cu(TMEDA)}]PF_6 (3). Complex **2** (30 mg, 0.034 mmol) and [Cu(*N*,*N*,*N*′,*N*′-tetramethylethylenediamine)$(NO_3)_2$] ([Cu(TMEDA)$(NO_3)_2$]) (23.6 mg, 0.0686 mmol) were dissolved into methanol (10 mL). To the solution was added NEt_3 (19 μL), and the mixture was stirred for 30 min. The resultant chestnut-colored solution was filtered. To the filtrate was added $TBAPF_6$ (66.5 mg, 0.172 mmol), and the solution was concentrated to a small volume to obtain a dark brown powder of **3**, which was washed with a minimum volume of CH_3CN and then dried. The yield was 52% (16.2 mg). ESI-MS: *m*/*z* 906.1 ([RuCl($(HCat)_2$-TPA){Cu(TMEDA)}]$^+$). Absorption maxima (λ_{max}, nm): 276 ($\varepsilon = 4.6 \times 10^4\ M^{-1}\ cm^{-1}$), 360 ($\varepsilon = 3.0 \times 10^4\ M^{-1}\ cm^{-1}$). The sample for the elemental analysis was prepared by precipitation with the addition of NH_4PF_6 instead of $TBAPF_6$ from the above filtrate due to the crystallization problem. The addition of slightly acidic NH_4PF_6 caused a protonation of the complex. Anal. Calcd for $C_{32}H_{27}N_6O_6RuClCuC_6H_{16}N_2 \cdot 2PF_6 \cdot CH_3OH \cdot H_2O$: C, 37.00; H, 3.82; N, 8.85. Found: C, 37.29; H, 3.60; N, 8.55.

X-Ray Crystallography on Complex 2′. A single crystal of the chloride salt, [RuCl(**L2**)]Cl·H_2O (**2′**), was obtained by recrystallization from CH_3OH/THF (see Table 1 for crystallographic details).[13] The crystal was mounted on a glass capillary with silicon grease and immediately cooled down to 93 K. All measurements were performed on a Rigaku Mercury CCD

Table 1. X-Ray Crystallographic Data for [RuCl(**L2**)]Cl (**2′**)

	2′
formula	$C_{32}H_{30}N_6O_7Cl_2Ru$
fw	782.60
cryst syst	monoclinic
space group	$P2_1/c$ (No. 14)
T, K	93
a, Å	13.1592(2)
b, Å	16.1463(3)
c, Å	18.4551(7)
β, deg	97.0165(8)
V, Å^3	3891.8(2)
Z	4
no. of reflns measured	7156
no. of observations	5351
no. of params refined	441
$R1$[a]	0.078 ($I > 2.0\sigma(I)$)
Rw[b]	0.216 ($I > 2.0\sigma(I)$)[c,d]
GOF	1.03

[a] $R1 = \sum||F_o| - |F_c||/\Sigma|F_o|$. [b] $Rw = [\sum(w(F_o^2 - F_c^2)^2)/\sum w(F_o^2)^2]^{1/2}$. [c] $w = 1/(\sigma^2(F_o))$. [d] $w = 1/[\sigma^2(F_o^2) + (0.1126P)^2 + 9.5888P]$, where $P = (\mathrm{Max}(F_o^2, 0) + 2F_c^2)/3$.

diffractometer at 93 K with graphite-monochromated Mo Kα radiation ($\lambda = 0.71070$ Å) up to $2\theta_{max} = 55.0°$.

The structure was solved by direct methods and expanded using Fourier techniques. All non-hydrogen atoms were refined anisotropically except two disordered Cl^-'s having 0.5 populations for each. Refinement was carried out with full-matrix least-squares on F with scattering factors from ref 14 and including anomalous dispersion effects. All calculations were performed using the Crystal Structure crystallographic software package,[15] and structure refinements were made by using SHELX-97.[16]

Electrochemical Measurements. Cyclic voltammetry (CV) and differential pulse voltammetry (DPV) measurements were performed at 298 K on an ALS electrochemical analyzer in deaerated MeCN (**1**) and DMF (**2** and **3**) containing 0.1 M [(*n*-Bu)$_4$N]ClO$_4$ (TBAP) or [(*n*-Bu)$_4$N]PF$_6$ (TBAPF$_6$) as a supporting electrolyte. A conventional three-electrode cell was used with a platinum working electrode (surface area of 0.3 mm^2) and a platinum wire as the counter electrode. The Pt working electrode (BAS) was routinely polished with an alumina suspension and rinsed with acetone before use. The measured potentials were recorded with respect to the Ag/AgNO$_3$ (0.01 M) reference electrode. All potentials (vs Ag/Ag$^+$) were converted to values vs SCE by adding 0.29 V.[17]

ESR Measurements. The ESR spectrum of **3** in distilled MeOH was recorded on a JEOL X-band spectrometer (JES-RE1XE) with a quartz ESR tube (4.5 mm i.d.) at 77 K. The ESR spectrum was measured under nonsaturating microwave power conditions. The magnitude of modulation was chosen to optimize the resolution and the signal-to-noise (S/N) ratio of the observed spectrum. The g values were calibrated with a Mn^{2+} marker.

Scheme 2. Synthesis of **L1** and **L2**

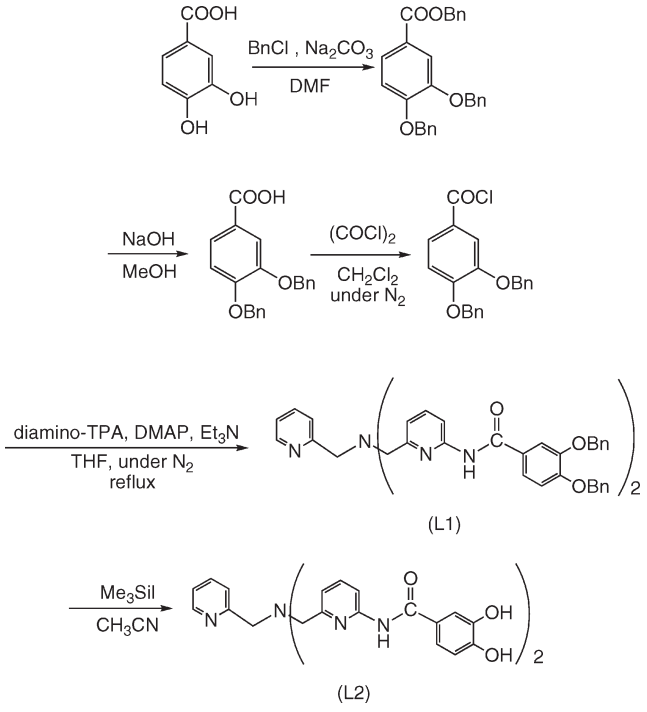

DFT Calculations. Density functional theory (DFT) calculations on the Ru−Cu complexes were carried out at the B3LYP[18]/LANL2DZ level of theory using the Gaussian 03 program.[19] The Los Alamos ECP with double-ζ basis for the Ru and Cu atoms[20] and the D95 basis set with standard double-ζ basis for other atoms[21] were used. To look in detail at the weak π−π interaction between the catechol moieties, second-order Mφller−Plesset perturbational (MP2)[22] calculations were performed for structures optimized at the B3LYP/LANL2DZ level of theory.

Results and Discussion

Synthesis of Ligands. The synthesis of the ligands was made in accordance with Scheme 2. In order to introduce catechol moieties to TPA, we first synthesized a benzyl-protected catechol derivative, 3,4-bis(benzyloxy)benzoic acid, that was converted quantitatively to the corresponding acid chloride by using oxalyl chloride. The reaction of *N*,*N*-bis(6-amino-2-pyridylmethyl)-*N*-(2-pyridylmethyl)-amine (diamino-TPA) with the acid chloride in the presence of 4-*N*,*N*-dimethylaminopyridine (DMAP) as a catalyst and triethylamine (NEt$_3$) as a base in THF gave *N*,*N*-bis[6-{3, 4-bis(benzyloxy)-benzamide}-2-pyridylmethyl]-*N*-(2-pyridylmethyl)amine ((Bn$_2$Cat)$_4$-TPA, **L1**) as a precursor in 50% yield. This compound was deprotected mildly in the presence of trimethylsilyl iodide to give the target compound, *N*,*N*-bis{6-(3,4-dihydroxybenzamide)-2-pyridylmethyl}-*N*-(2-pyridylmethyl)amine ((H$_2$Cat)$_2$-TPA; **L2**) in 85% yield.

(13) We could not obtain enough amount of the complex to attain its elemental analysis data; however, the structure determined did not show any discrepancy with the spectroscopic data of the corresponding PF_6^- salt. Thus, we concluded that the structure of the PF_6^- salt should be the same as the Cl^- salt.

(14) Creagh, D. C.; McAuley, W. J. *International Tables for Crystallography*; Wilson, A. J. C., Ed.; Kluwer Academic Pulishers: Boston, 1992; Vol. *C*, Table 4.2.6.8, pp 219−222.

(15) *CrystalStructure 3.7.0: Crystal Structure Analysis Package*; Rigaku and Rigaku/MSC: The Woodlands, TX, 2000−2005.

(16) Sheldrick, G. M. *SIR 97 and SHELX 97, Programs for Crystal Structure Refinement*; University of Göttingen: Göttingen, Germany, 1997.

(17) Mann, C. K.; Barnes, K. K. *Electrochemical Reactions in Nonaqueous Systems*; Marcel Dekker: New York, 1990.

(18) (a) Becke, A. D. *Phys. Rev. A* **1988**, *38*, 3098. (b) Becke, A. D. *J. Chem. Phys.* **1993**, *98*, 5648. (c) Lee, C.; Yang, W.; Parr, R. G. *Phys. Rev. B* **1988**, *37*, 785. (d) Vosko, S. H.; Wilk, L.; Nusair, M. *Can. J. Phys.* **1980**, *58*, 1200. (e) Stephens, P. J.; Devlin, F. J.; Chabalowski, C. F.; Frisch, M. J. *J. Phys. Chem.* **1994**, *98*, 11623.

(19) Frisch, M. J. et al. *Gaussian 03*, revision C.02; Gaussian, Inc.: Wallingford, CT, 2004. The full list of authors is given in the Supporting Information.

(20) Dunning, T. H.; Hay, P. J. In *Modern Theoretical Chemistry*; Schaefer, H. F., III, Ed.; Plenum: New York, 1976; Vol. *3*, p 1.

(21) Hay, P. J.; Wadt, W. R. *J. Chem. Phys.* **1985**, *82*, 270.

(22) Mfller, C.; Plesset, M. S. *Phys. Rev.* **1934**, *46*, 618.

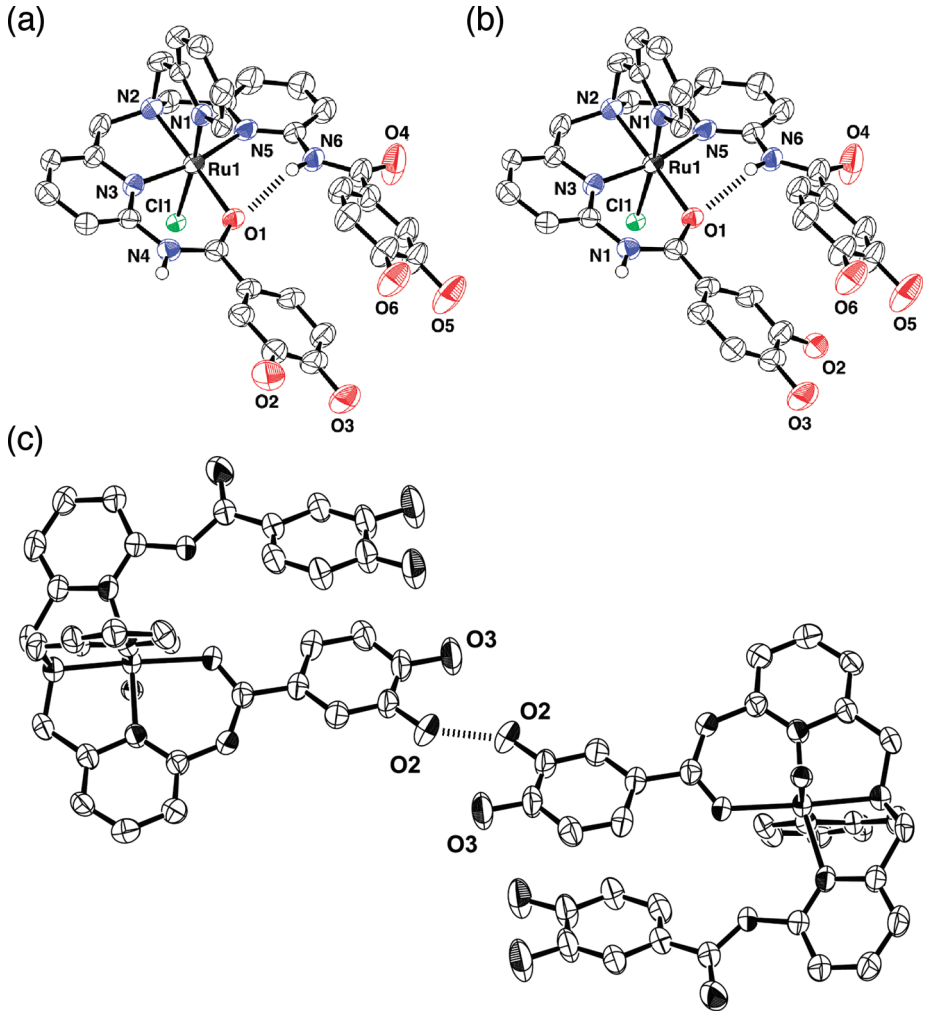

Figure 1. ORTEP drawings the cation moiety of **2′**: two isomers A (a) and B (b). (c) Intermolecular hydrogen bonding between two adjacent catechol moieties for isomer A. Hydrogen atoms are omitted for clarity except the amide N−H hydrogen atoms in A and B.

Synthesis of Ru(II) Complexes of L1 (1) and L2 (2). We have reported on the synthesis of bisamide-TPA with various functional groups and their Ru(II) complexes by using $RuCl_3 \cdot 3H_2O$ or $[RuCl_2(DMSO)_4]$ as a metal source.[9,10] On the basis of that, the reaction of **L1** with $RuCl_3 \cdot 3H_2O$ in ethanol as reported previously gave a Ru(II) complex of **L1**, [RuCl(**L1**)]PF_6 (**1**), in 58% yield. However, the preparation of a Ru(II) complex of **L2** was not successful with the use of those starting materials previously used. Thus, we changed the starting material to a bis-μ-chloro dinuclear precursor complex, $[RuCl_2(p\text{-cymene})]_2$, and the reaction of **L2** with the precursor was performed in methanol at reflux for 24 h. The reaction proceeded smoothly to give an orange solution, and the addition of NH_4PF_6 afforded [RuCl(**L2**)]PF_6 (**2**) as a reddish orange precipitate in 56% yield.

In this synthetic reaction, the characteristics of the Ru(II) ion play an indispensable role for its selective binding to the TPA moiety rather than the catechol moieties. The Ru(II) ion favors heteroaromatics due to stabilization of their coordination by π-back-bonding from the filled d_π orbitals (t_{2g}) to the π^* orbitals of heteroaromatics in addition to their σ-bonding by σ-donation of the lone pair(s) to the empty d_σ orbital (e_g) of Ru(II). The catechol oxygen is categorized into the "hard" base;[23] therefore, the Ru(II) coordination occurs at the TPA unit preferentially over that at the catechol moieties. Thus, we could obtain complex **2** in moderate yield.

Crystal Structure of Complex 2′. Recrystallization of a powder of **2** from CH_3OH/THF gave a single crystal of an unexpected chloride salt, [RuCl(**L2**)]$Cl \cdot H_2O$ (**2′**), which was suitable for X-ray crystallography to establish its molecular structure. ORTEP drawings of the cation moiety of **2′** are depicted in Figure 1 with partial numbering scheme. As can be seen in the figure, **L2** coordinates to the Ru(II) center as a pentadentate ligand including an amide oxygen. We found disorder of the catechol moiety including O2 and O3 to conclude that the crystal contained two isomers A and B in terms of the direction of the catechol moiety linked to the coordinated amide arm as shown in Figure 1a and b, respectively.

The Ru(II) center possesses an octahedral geometry and one of the amide oxygen atoms in **L2** coordinates to the Ru(II) ion at the position *trans* to the tertiary amino group of **L2**. The bond length between the chloride anion

(23) (a) Huheey, J. E.; Keiter, E. A.; Keiter, R. L. *Inorgic Chemistry*, 4th ed.; HarperCollins College Publisher: New York, 1993; pp 344−355. (b) Pearson, R. G. *J. Am. Chem. Soc.* **1963**, *85*, 3533–3539.

Table 2. Selected Bond Lengths (Å) and Angles (deg) of **2′**

Ru1−Cl1 2.505(1)	Ru1−O1 2.088(4)
Ru1−N1 2.032(4)	Ru1−N2 2.045(5)
Ru1−N3 1.993(4)	Ru1−N5 2.103(5)
Cl1−Ru1−N1 175.0 (1)	O1−Ru1−N3 90.1(2)
O1−Ru1−N5 103.5(2)	O1−Ru1−N2 175.0(2)
N1−Ru1−N2 82.3(2)	N2−Ru1−N3 86.2(2)
N2−Ru1−N5 86.4(2)	N3−Ru1−N5 166.3(2)

and the Ru(II) ion is 2.505(1) Å (see Table 2), which is longer than those found in other $[RuCl(bisamide\text{-}TPA)]^+$ reported so far. The amide oxygen binds to the Ru(II) center in the distance of 2.088(4) Å, which is a little shorter than those in other related Ru(II)−bisamide−TPA complexes.[9b,10] The dissymmetry for the bond lengths of Ru1−N3 (1.993(4) Å) and Ru1−N5 (2.103(5) Å), which are *trans* to each other, is also typical for the Ru−(bisamide−TPA) complexes, due to chelation of the amide moiety to make the N3 atom strongly interact with Ru1 and steric requirements for the two neighboring functional groups to hold the appropriate distance.

In each isomer, the two catechol moieties exhibit intramolecular $\pi-\pi$ interaction with interatomic distances of 3.42 and 3.51 Å. The catechol oxygen atoms of O3 in the isomer A and O2 and O3 in the isomer B form hydrogen bonds with water molecules of crystallization. In addition to the hydrogen bonding with water molecules of crystallization, the O2 atom of the catechol moiety in the isomer A showed intermolecular hydrogen bonding with each other in the crystal, as shown in Figure 1c.

In addition, the amide N−H of the uncoordinating amide arm directs to the coordinated amide oxygen in the coordinating amide arm, forming intramolecular hydrogen bonding with the interatomic distance of 2.938(7) Å for O1···N6 and the angle of 148.9(4)° for O1···H−N6 to stabilize the structure as observed in other related complexes.[9a,b]

Spectroscopic Characterization of Ru(II) Complexes. Complex 1. Complex 1. The ESI-MS spectrum of **1** in MeCN showed a peak cluster assigned to $[RuCl((Bn_2\text{-}Cat)_2\text{-}TPA)]^+$ (m/z = 1089.3), and its isotopic pattern of the spectrum was consistent with the computer simulation.

The ^{1}H NMR spectrum (300 MHz) of **1** in CD_3CN showed three AB quartets assigned to the methylene protons at 4.34 and 4.47 ppm (J_{AB} = 18 Hz), 4.64 and 4.95 ppm (J_{AB} = 15 Hz), and 4.65 and 5.14 ppm (J_{AB} = 14 Hz). These indicate that one of the amide oxygen atoms coordinates to the ruthenium center to hold an asymmetric structure in MeCN. A doublet at 8.45 ppm (J = 5 Hz) was assigned to axial pyr−H6, because the typical coupling constant of the axial pyr−H6 of other Ru(II) complexes with TPA derivatives was about 5 Hz.[24] Assignments for other aromatic protons were not possible due to severe overlap of signals. Singlet peaks assigned to the CH_2 groups of the benzyl arms were observed at 4.78, 5.03, 5.08, and 5.12 ppm, reflecting the asymmetric coordination environment.

The UV−visible spectrum of **1** in MeCN showed an MLCT band from Ru(II) to pyridine at 305 nm and an LMCT band from Cl^- to Ru(II) at 455 nm. Upon the addition of 1 equiv of NEt_3, the orange solution turned reddish orange and the absorption spectrum changed to show an increase in the intensity of the absorption of the LMCT band (see Supporting Information). This change is similar to that observed for $[RuCl((1\text{-}Naph)_2\text{-}TPA)]PF_6$,[9b] but with a smaller magnitude. The original spectrum was recovered by adding 1 equiv of $HClO_4$. Thus, this reversible spectral change by adding base and acid is attributed to reversible deprotonation and protonation of the coordinated amide moiety as shown in Scheme 3.

Scheme 3. Reversible Deprotonation−Protonation Reaction of **1**

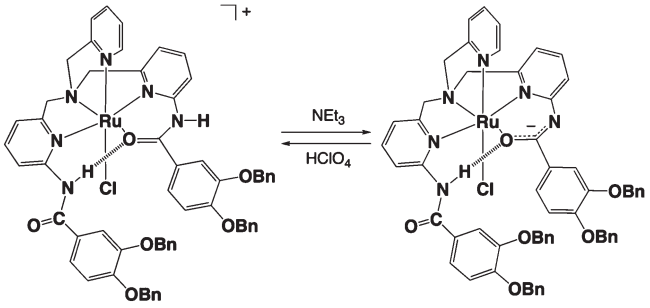

Complex 2. The ESI-MS spectrum of **2** in MeOH was measured to observe a peak cluster assigned to $[RuCl(\mathbf{L2})]^+$ at m/z = 729.2 with a specific isotopic pattern for a mononuclear ruthenium complex. This mass number is consistent with that calculated for the cation moiety of **2**, and the computer-simulated isotopic pattern of the mass spectrum shows good agreement with the observed one. The result of elemental analysis also exhibited good agreement with the calculated values for $\mathbf{2}\cdot 4H_2O\cdot CH_3CN$.

The ^{1}H NMR spectrum of **2** was measured in CD_3CN. First of all, the peaks assigned to the methylene protons of the TPA moiety were observed in the range of 4 to 5 ppm, and they were split into three AB quartets: 4.34 and 4.53 ppm (J_{AB} = 18 Hz), 4.48 and 4.58 ppm (J_{AB} = 18 Hz), and 4.75 and 4.90 ppm (J_{AB} = 15 Hz). This is indicative of the coordination of one of the amide oxygen atoms in **L2** to the Ru(II) center in addition to the tetradentate TPA moiety as well as complex **1** and other structurally characterized Ru(II) complexes bearing pentadentate bisamide−TPA ligands. A relatively sharp singlet at 9.81 ppm was assigned to the uncoordinated amide N−H, which forms intramolecular hydrogen bonding with the coordinated amide oxygen, and a broad singlet at 10.05 ppm was ascribed to the N−H in the coordinated amide linkage, as reported previously.[9b,25] Other peaks can be assigned by using ^{1}H−^{1}H COSY spectroscopy. It should be noted that the product obtained is only one species on the bases of NMR measurements, in contrast to the fact that the two isomeric structures were found in the crystal as depicted in Figure 1. Two doublet peaks observed at 6.39 and 6.67 ppm were assigned to those of the uncoordinated catecholamide moiety, and these signals exhibited upfield shifts relative to those observed for **L2** by more than 0.4 ppm. This clarifies the fact that the 5 and 6 positions of the catechol moiety connected to

(24) Kojima, T.; Amano, Y.; Ishii, M.; Ohba, Y.; Okaue, Y.; Matsuda, Y. *Inorg. Chem.* **1998**, *37*, 4076–4085.

(25) In DMSO-d_6, we could observe singlets due to OH groups of the catechol moieties in the range of 9.36−9.96 ppm.

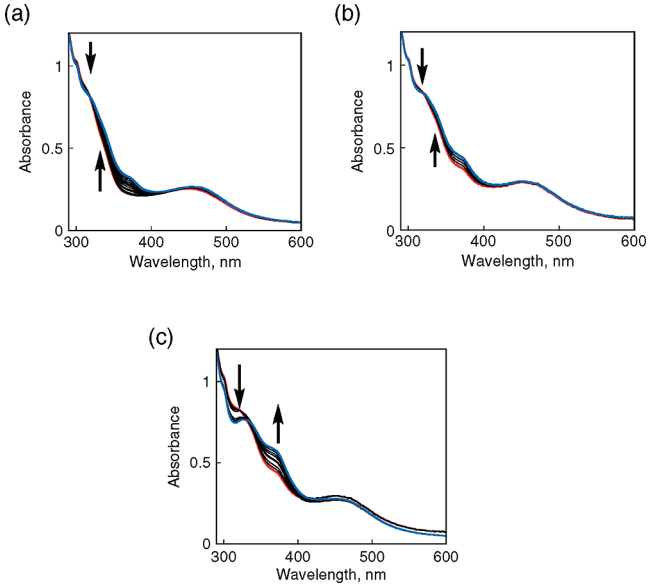

Figure 2. Absorption spectral change of **2** in the course of the addition of TMAOH in DMF: (a) 0−2 equiv; (b) 2−3 equiv; (c) 3−5 equiv. Arrows indicate the directions of absorbance changes.

the uncoordinated amide linkage experience the ring current of the counterpart, indicating the existence of the intramolecular $\pi-\pi$ interaction between the two catechol moieties in **2**. This situation holds for both isomer A and isomer B, as can be seen in Figure 1, precluding a definitive standpoint to nail down the species observed in the NMR spectrum in CD_3CN.

MP2 calculations were performed to evaluate the energy difference between the two isomers A and B optimized at the B3LYP/LANL2DZ level of theory (see the Supporting Information). Isomer B was calculated to be more stable than isomer A by 1.9 kcal/mol. This energy difference corresponds to the population ratio of A/B being 4:96, suggesting that the species observed in the NMR spectrum could be isomer B. The interatomic distances of the catechol moieties in the optimized structure of isomer B were slightly shorter than those of isomer A. Such stronger intramolecular $\pi-\pi$ interaction of the catechol moieties can be a major factor of stabilization for isomer B compared to isomer A.

In the absorption spectrum of **2** in MeOH, an LMCT band, which was assigned to that from Cl^- to Ru(II) as a main factor, was observed at 442 nm. A similar LMCT band was observed for $[Ru^{II}Cl(\text{bisamide-TPA})]^+$. Upon the addition of tetramethylammonium hydroxide (TMAOH) to the DMF solution of **2**, we could observe three-step spectral change. In the course of the addition of 0−2 equiv of TMAOH, the spectrum changed, exhibiting an isosbestic point at 318 nm as depicted in Figure 2a. The LMCT band exhibited a slight red shift to give the absorption maximum at 458 nm, and a new absorption emerged at 369 nm. This spectral change accompanying the red shift of the LMCT band can be ascribed to the deprotonation of the coordinated N−H proton as observed for other Ru(II)−(bisamide-TPA) complexes mentioned above. It has been reported that the pK_a values of catechols having amide groups are $pK_{a1} \sim 8$ and $pK_{a2} \sim 13$.[26] The coordination of the amide oxygen attached to the catechol results in lowering the pK_a values. Together with the fact that the pK_a value of the coordinated amide moiety has been estimated to be ~6 for $[RuCl((1\text{-Naph})_2\text{-TPA})]^+$ ((1-Naph)$_2$-TPA = *N*,*N*-bis{6-(1-naphthoylamide)-2-pyridylmethyl}-*N*-(2-pyridylmethyl)amine) in a CH_3CN/Britton-Robinson buffer,[9b] we assume that the coordinated amide N−H proton and one of the catechol O−H protons are simultaneously deprotonated at this stage. This suggests that one of the four catechol O−H protons in **2** should be discriminated in terms of acidity. The second spectral change was observed in the course of the addition of 2−3 equiv of TMAOH in total, showing an isosbestic point at 320 nm as depicted in Figure 2b. In this step, only one proton was removed. Another discriminated proton would exist in **2**, and its acidity should be lower than the former. The final step required two more equivalents (3−5 equiv) of TMAOH to exhibit no further spectral change with an isosbestic point at 332 nm as shown in Figure 2c. At this stage, the absorption at 369 nm gained further intensity. This step can be attributed to the deprotonation of the least acidic protons of catechols, that is, a chelated proton between the two oxygen atoms. On the basis of these observations, we propose an intramolecular hydrogen bonding network between the two converged catechols in **2** as depicted in Scheme 4.

Complexation of 2 with a Cu(II)−Diamine Unit. The complexation capability of the preorganized catechols of **2** was examined by using a Cu(II)−diamine unit: In the Irwing−Williams series, Cu(II) has been demonstrated to form the most stable complexes with a bidentate chelating ligand to afford a five-membered chelate ring.[27] Thus, we chose $[Cu^{II}(NO_3)_2(\text{TMEDA})]$ (TMEDA = *N*,*N*,*N*′*N*′-tetramethylethylenediamine)[11] as a precursor, having two coordinatively labile sites to facilitate the catechol binding. No reaction of **2** with the precursor in MeOH occurred in the absence of a base. Upon the addition of NEt_3 into the solution, the reaction proceeded smoothly with a color change to exhibit a chestnut color in the solution. The addition of $TBAPF_6$ gave a dark brown powder of a new species, **3**.

The new species showed the absorption maxima at 276 and 360 nm. This complex **3** was submitted to ESI-MS measurements and was shown to exhibit a peak cluster at m/z = 906.1, which was assigned to $[RuCl((HCat)_2\text{-TPA})\{Cu(\text{TMEDA})\}]^+$.[28] The computer simulation gave rise to an excellent agreement with the isotopic pattern and mass number, as shown in Figure 3. On the basis of this result, this complex is a monocation, including only one Cu(II)-TMEDA unit in spite of the fact that **2** contains two distinct catechol moieties.

The titration was performed by adding $[Cu(NO_3)_2\text{-}(\text{TMEDA})]$ to the solution of **2** in MeOH to determine

(26) (a) Arnould, J. C.; Bertrandie, A.; Bird, T. G. C.; Boucherot, D.; Jung, F.; Lohmann, J. J.; Olivier, A. *J. Med. Chem.* **1992**, *35*, 2631–2642. (b) Paulini, R.; Lerner, C.; Diederich, F.; Jakob-Roetne, R.; Zürcher, G.; Borroni, E. *Helv. Chim. Acta* **2006**, *89*, 1856–1887. (c) El Hage Chahine, J.-M.; Bauer, A.-M.; Baraldo, K.; Lion, C.; Ramiandrasoa, F.; Kunesch, G. *Eur. J. Inorg. Chem.* **2001**, 2287–2296.

(27) Huheey, J. E.; Keiter, E. A.; Keiter, R. L. *Inorganic Chemistry*, 4th ed.; HarperCollins College Publisher: New York, 1993; pp 348−349.

(28) When NH_4PF_6 was used in place of $TBAPF_6$ in the purification process, a protonated form of **3**, $[RuCl((HCat, H_2Cat)\text{-TPA})\{Cu(\text{TMEDA})\}](PF_6)_2$, was obtained. See the Experimental Section.

Scheme 4. Proposed Deprotonation Sequence for **2**

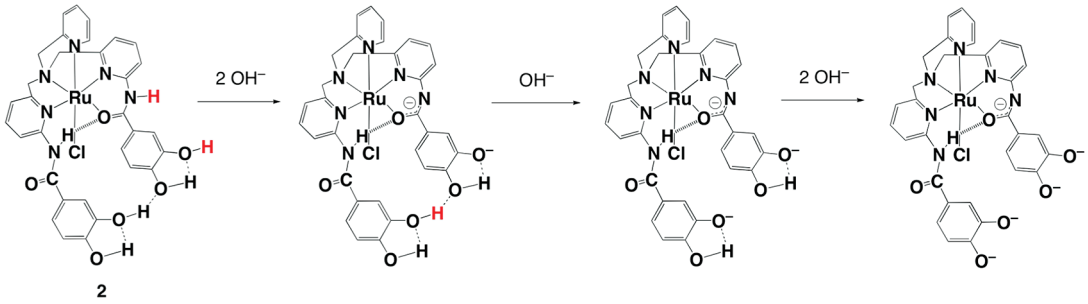

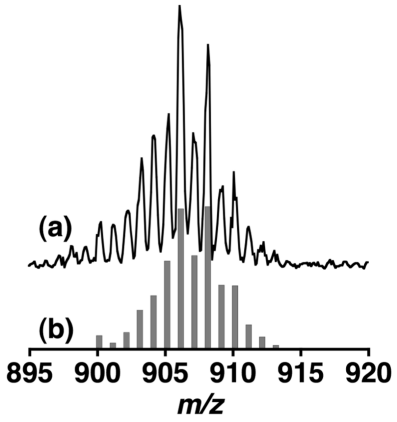

Figure 3. ESI-MS spectrum of **3**: (a) observed, (b) simulated isotopic pattern.

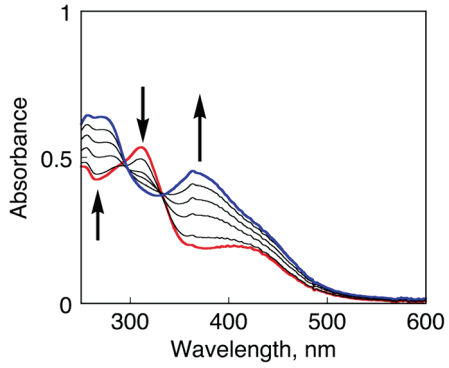

Figure 4. Absorption spectral change of **2** in MeOH in the course of the addition of 1 equiv of $[Cu(NO_3)_2(TMEDA)]$ in the presence of an excess amount of NEt_3. Red line, **2**; black lines, 0.2−0.8 equiv addition of $[Cu(NO_3)_2(TMEDA)]$; blue line, 1 equiv of $[Cu(NO_3)_2(TMEDA)]$.

the number of Cu(II)-TMEDA units to be allowed to bind to the catechol moieties in **2**. We could observe drastic spectral change in the course of the addition of 1 equiv of the Cu(II) complex, as shown in Figure 4; however, no additional change was observed in its further addition. Thus, we concluded that the convergent catechol moieties could accept only one Cu(II) unit. This result should be relevant to that in the titration of **2** with TMAOH: After one proton is removed, another discriminated proton is deprotonated, as depicted in Scheme 4.

The ESR spectrum of **3** (1.0×10^{-5} M) in MeOH solution at 77 K is shown in Figure 5a. As a comparison,

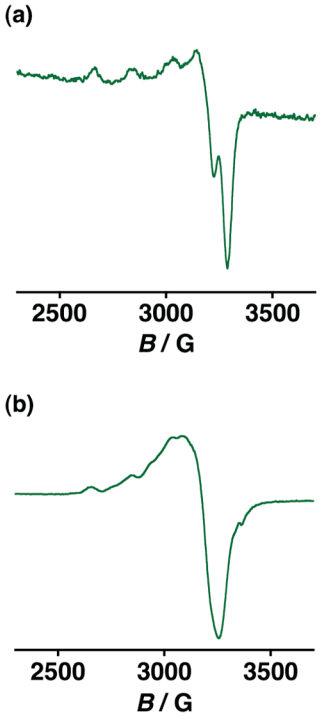

Figure 5. ESR spectra of **3** (a) and [Cu(catecholato)(TMEDA)] (b) in MeOH at 77 K. Conditions: Microwave power, 1 mW; 100 kHz modulation amplitude, 2 mT; frequency, 9.203 GHz (a) and 9.208 GHz (b).

[Cu(catecholato)(TMEDA)][29] (Cu^{II}−catecholate) was synthesized to measure its ESR spectrum (Figure 5b). In the complex **3**, the $g_{||}$ and $g_{\perp}$ values are 2.239 and 2.060, respectively, with a hyperfine coupling constant for Cu(II) of $A_{||} = 184$ G. In the Cu^{II}−catecholate, the $g_{||}$ and $g_{\perp}$ values are 2.241 and 2.071, respectively, and the hyperfine coupling constant $A_{||}$ is 184 G as shown in Figure 5b. In both cases, the ESR signals of Cu(II) centers indicate that the Cu(II) centers in both complexes are with a monomeric tetragonal geometry in the $(d_{x^2-y^2})^1$ ground state.[30] These observations indicate that the Cu(II) center in **3** is in a different environment from that of the Cu-catecholate and support the unique coordination described in Scheme 5.

DFT calculations were performed for the structure optimization of **3**. The optimized structure is depicted in Figure 6. This structure is more stable by −3.5 kcal/mol in terms of the heat of formation than that including the *O*,

(29) Kodera, M.; Kawata, T.; Kano, K.; Tachi, Y.; Itoh, S.; Kojo, S. *Bull. Chem. Soc. Jpn.* **2003**, *76*, 1957–1964.

(30) (a) Wojciechowski, K.; Bitner, A.; Bernardinelli, G.; Brynda, M. *Dalton Trans.* **2009**, 1114–1122. (b) Nielsen, P.; Toftlund, H.; Boas, J. F.; Pilbrow, J. R.; Moubaraki, B.; Murray, K. S.; Neville, S. M. *Inorg. Chim. Acta* **2008**, *361*, 3453–3461.

Scheme 5. Complexation of the Cu(II)-TMEDA Unit with **2**

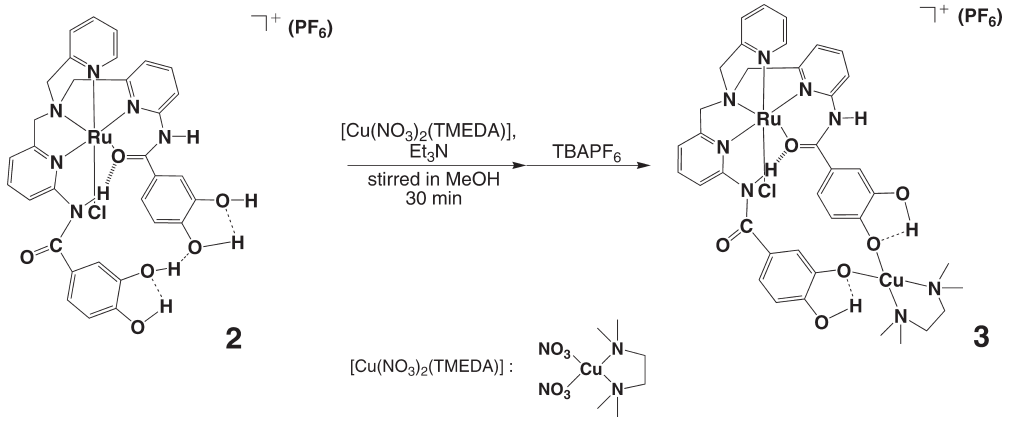

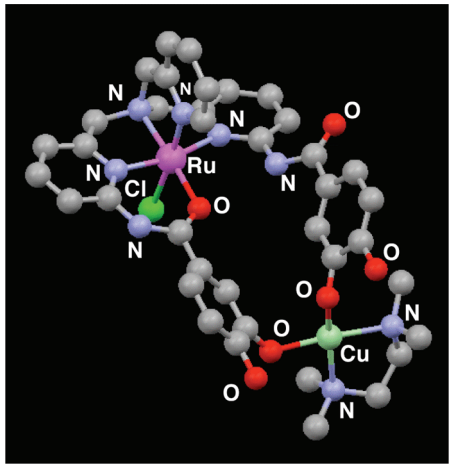

Figure 6. DFT-optimized structure of **3** at the B3LYP/LANL2DZ level of theory. Hydrogen atoms are omitted for clarity.

O′-bidentate chelation of the catechol moiety with the coordinated amide linkage to the Cu(II)-TMEDA unit (see Supporting Information). In this structure, the catechol moieties are tilted from the coordinated amide−pyridine plane to bind the square-planar Cu(II)-TMEDA fragment. The bond lengths of Cu(II)−O(cat) were calculated to be 1.933 and 1.968 Å, and the bond angle of O−Cu−O was 92.0°. Those bond lengths are fairly longer than typical values for Cu(II)−O (terminal aryloxy) bonds in a four-coordinate Cu(II) complex.[31] The long Cu−O bond lengths are probably derived from significant distortion of the catechol−amide−pyridine skeletons, as mentioned above, to accommodate the square planar coordination environment of the Cu(II) center.

Summary

We have described the synthesis and characterization of Ru-TPA complexes bearing catechol moieties connected by amide linkages. In the ruthenium complex with catechol moieties (**2**), there is intramolecular $\pi-\pi$ interaction between the two catechol moieties due to their convergence by virtue of the preorganization of those functional groups. This convergence could be achieved by a template effect of the selective coordination of Ru(II) to the TPA moiety of the ligand. In addition to the intramolecular $\pi-\pi$ interaction, the catechol moieties have been suggested to form a plausible intramolecular hydrogen bonding network, which gives rise to the selective formation of one isomer out of four possible isomers in terms of orientation of the two catechol moieties.

The converged catechol moieties on the surface of the Ru(II) complex can act as a metal−complex ligand. We could confirm the coordination of a copper−diamine unit to the catechol site. The number of Cu(II) allowed to bind is restricted to only one, even though two chelatable catechols should be ready to form stable five-membered chelate ring structures. Thus, we propose that the coordination of the Cu(II)-diamine unit to the converged moieties is in a novel coordination mode, such as a bridging mode between the two catechol moieties to form a unique binuclear Ru(II)−Cu(II) complex with multiredox centers and proton-transfer sites. This complex can provide a new frontier and a new basis of development of novel electronic structures of multinuclear transition metal complexes to afford their interesting properties and reactivities.

Acknowledgment. This work was supported by Grants-in-Aid (No. 16550057, 19205019, 20108010) from Japan Promotion of Science and Technology (JSPS), a Global COE program, "The Global Education and Research Center for Bio-Environmental Chemistry", from MEXT, Japan, and by KOSEF/MEST through the WCU project (R31-2008-000-10010-0). S.M. appreciates the support from a JSPS postdoctoral fellowship (no. 10727).

Supporting Information Available: Crystallographic data of 2′ in the cif format, UV−vis spectral change of **1** with the addition of NEt_3 and $HClO_4$, CV change of **1** upon the addition of NEt_3, DFT-optimized structures of the isomers A and B in Figure 1, another possible Cu(II)-TMEDA adduct, and ^1H NMR spectra of **1** and **2**. This material is available free of charge via the Internet at http://pubs.acs.org.

(31) Guy Orpen, A.; Brammer, L.; Allen, F. H.; Kennard, O.; Watson, D. G.; Taylor, R. *J. Chem. Soc., Dalton Tans.* **1989**, S1–S83.